

# Field-Deployable Hybrid Gravimetry: Projecting Absolute Accuracy Across a Remote 24km<sup>2</sup> Survey via Daily Quantum Calibration

Nathan Shettell,<sup>1,†</sup> Kai Sheng Lee,<sup>1,†</sup> Fong En Oon,<sup>1</sup>  
Elizaveta Maksimova,<sup>1</sup> Hong Hui Chen,<sup>1</sup> and Rainer Dumke<sup>1,2</sup>

<sup>1</sup>*Centre for Quantum Technologies, National University of Singapore, Singapore 117543, Singapore*

<sup>2</sup>*School of Physical and Mathematical Sciences, Nanyang Technological University, 637371, Singapore*

Absolute gravimeters deliver drift-free, high-precision measurements but are typically bulky and difficult to deploy, whereas relative gravimeters are lightweight and mobile but intrinsically limited by time-dependent drift. We demonstrate a hybrid quantum-enabled gravimetry approach in which an on-site atomic gravimeter provides routine,  $\mu\text{Gal}$ -level calibration of two mobile spring gravimeters during a field survey spanning 24 km<sup>2</sup> of dense tropical terrain. The atomic reference enables high-precision, asynchronous cross-comparison of relative measurements acquired over seven days, effectively suppressing instrumental drift to a level required for demanding geophysical applications. This deployment captures regional gravity gradients with high fidelity under challenging environmental conditions, illustrating how field-operable quantum sensors can extend quantum-grade gravimetry beyond laboratory settings and serve as scalable calibration backbones for large-area, high-precision geophysical surveys in remote or logistically constrained environments.

Gravimetry is a cornerstone of subsurface investigation, providing a passive and non-invasive probe of density variations beneath the Earth’s surface [1–3]. Because gravitational fields cannot be shielded or attenuated, gravity measurements can reveal geological structures inaccessible to electromagnetic or acoustic methods [1, 4, 5]. As a result, reference-free precision gravimetry plays a critical role in applications ranging from groundwater monitoring and crustal deformation studies to long-term environmental observation [6–8].

Field gravity surveys are traditionally performed using either relative or absolute gravimeters [5]. Relative instruments, including spring-based gravimeters, are compact and well suited to dense spatial sampling, but rely on internal references that introduce time-dependent drift and sensitivity to environmental conditions [9–11]. Absolute gravimeters, by contrast, measure gravitational acceleration directly in SI units and provide intrinsically drift-free references [5, 12]. In particular, atomic gravimeters exploit quantum effects of ultracold atoms such as matter-wave interference achieve high precision, long-term stability [13–16]. These quantum sensors represent a major advance in gravimetry, but their complexity, environmental sensitivity, and deployment footprint have so far limited their routine use in large-area field surveys [17–21].

Hybrid gravimetry has recently emerged as a promis-

ing strategy to bridge this gap by combining mobile relative gravimeters with an absolute reference [20–29]. In this approach, an absolute gravimeter provides calibration that suppresses drift in relative instruments while preserving their operational flexibility. Here, we extend this concept by deploying a compact atomic gravimeter as a continuously operating quantum reference during a large-area field survey. We report results from a hybrid gravity survey conducted over a 24 km<sup>2</sup> region of dense tropical terrain, where environmental variability and limited infrastructure posed significant challenges. Two CG6 Autograv spring gravimeters [30] were routinely cross-calibrated against the atomic gravimeter throughout the campaign, enabling microGal-level drift correction and high-precision asynchronous measurements over multiple days. This work demonstrates the viability of field-deployed quantum gravimeters as calibration backbones for scalable, high-precision gravity surveys in demanding environments.

## METHODS

Prior to data collection, a site reconnaissance was conducted to identify a suitable location for the atomic gravimeter base station. Selection criteria were driven by both operational and metrological requirements: suf-

ficient space to house an air-conditioned cargo container for the quantum gravimeter ( $75\text{ cm} \times 75\text{ cm} \times 200\text{ cm}$ ), provision for continuous power via a generator, and mechanically stable, level ground to minimize tilt-induced bias over the duration of the deployment. The survey was confined to a  $24\text{ km}^2$  area of remote, forested terrain on an island off the coast of Singapore; the exact geographic coordinates are not disclosed.

The initial phase of the campaign (2–5 October 2023) was dedicated to installation, alignment, and stabilization of the atomic gravimeter. Field gravity measurements were subsequently conducted between 6 and 12 October 2023, with daily survey operations carried out between 10:00 and 17:00, weather permitting. Two CG6 spring gravimeters were used for mobile measurements and returned each evening to a fixed location adjacent to the atomic gravimeter base station. During overnight periods (approximately 18:00 to 09:00), both the atomic and spring gravimeters remained stationary and recorded continuous gravity data at one-minute intervals. Because all instruments sampled the same local gravitational field under stable conditions, these measurements provided a common reference for monitoring and correcting time-dependent drift in the relative gravimeters [11, 20]. This calibration scheme enabled high-precision cross-comparison between mobile measurements acquired on different days. The instrument configuration at the reference station is depicted in Fig. (1).

## Measurements

Two spring gravimeters were operated concurrently to measure local variations in gravitational acceleration along separate survey paths. Measurement stations were spaced at least 50m apart along predefined survey axes. At each station, the gravimeter was leveled by adjusting its tripod until the internal tilt readings were within  $\pm 10$  arcseconds, after which the instrument was observed for approximately 30 s to verify mechanical stability. If significant drift was detected—typically due to soft or uneven ground—the instrument was repositioned to a more stable surface and re-leveled. Once a stable setup was achieved, gravity data were acquired over a 5 min interval, with five measurements recorded

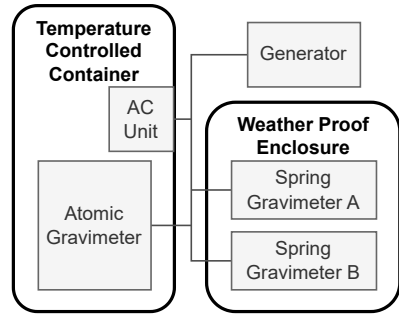


FIG. 1. Layout of the reference station used for daily calibration. The atomic gravimeter was housed inside an air-conditioned container (approximately  $75\text{ cm} \times 75\text{ cm} \times 200\text{ cm}$ ) and operated continuously to provide an absolute gravity reference, with the container positioned on a cemented clearing to ensure stability. Spring gravimeters were placed in a neighbouring weather-proof metal enclosure during overnight calibration periods, enabling correction for instrumental drift. A common generator provided electrical power throughout the survey.

at one-minute cadence.

## GPS

Precise latitude, longitude, and elevation information were required to resolve spatial variations in the gravity field and to compute terrain-related corrections, including Bouguer anomalies [31]. Dense canopy cover across much of the survey area limited satellite visibility, necessitating GPS measurements at locations with sufficient sky exposure. Each spring gravimeter was fitted with a rigid metal bracket supporting a GPS antenna, enabling position data to be recorded concurrently with each gravity measurement, while a continuously operating GPS receiver on a nearby building served as a fixed reference station for post-processed kinematic (PPK) analysis.

PPK processing combined reference-station and mobile-antenna data to refine the position estimates for each measurement. Solutions either achieved centimeter-level vertical precision, provided reduced or unquantified vertical accuracy, or failed to converge; only the latter were excluded from further anal-

ysis. Stations with centimeter-level precision provided high-quality elevation control for validating the atomic gravimeter as a stable temporal reference, while stations with reduced accuracy were retained to preserve spatial coverage and support analysis of longer-wavelength gravity variations across the survey area.

## DATA CORRECTION

Understanding gravity variations across the survey area requires careful correction for both temporal and spatial (elevation and terrain dependent) effects, ensuring that the residual gravity signal can be confidently attributed to subsurface mass distributions. In gravimetry, only horizontal variations are typically of interest, while vertical variations, instrumental drift, and tidal effects must be removed. Additionally, spring gravimeters measure relative gravity rather than absolute values, necessitating calibration against an absolute reference to ensure consistency across instruments and survey periods.

Without loss of generality, the spring gravimeter measurements at horizontal position  $\vec{x}$  (latitude and longitude) and time  $t$  can be expressed as

$$g_{\text{sg}}(\vec{x}, t) = g_0(\vec{x}) + \delta_t g(\vec{x}, t) + \delta_z g(\vec{x}) + \Delta_{\text{sg}}(t), \quad (1)$$

where

1.  $g_0(\vec{x})$  is the absolute gravity at position  $\vec{x}$ , which represents the desired signal after all corrections;
2.  $\delta_t g(\vec{x}, t)$  captures time-dependent variations in the gravity field at position  $\vec{x}$  arising from geophysical and environmental processes, e.g., tidal dynamics and ocean loading;
3.  $\delta_z g(\vec{x})$  accounts for elevation-dependent spatial corrections, such as free-air and Bouguer corrections applied to reference measurements;
4.  $\Delta_{\text{sg}}(t)$  represents instrument-specific, slowly varying temporal effects associated with the spring gravimeter, including bias offsets and long-term drift. Over short timescales this term is typically dominated by an approximately linear drift, and it is continuously constrained through calibration

against the atomic gravimeter to ensure faithful transfer of long-term gravity variations into the relative data.

In this analysis, all gravity measurements are referenced to mean sea level, as determined from GPS-derived elevations. Data correction is therefore divided into two components: i) *Temporal corrections*, addressing instrumental drift, tidal effects, and inter-instrument calibration; and ii) *Elevation corrections*, accounting for vertical variations in gravitational acceleration due to changes in elevation.

### Temporal Correction

Two primary sources of temporal variation in gravity measurements are Earth tides [32, 33] and instrumental drift in the spring gravimeters [11]. Tidal effects, which can reach amplitudes up to 150  $\mu\text{Gal}$ , were removed from both absolute and relative gravity data using the external model of Micro-g LaCoste' QuickTide Pro.

Instrumental drift was corrected using the continuously recording atomic gravimeter as an on-site absolute reference. Each evening, the spring gravimeters were co-located with the atomic instrument and left recording overnight under stable conditions (18:00–07:00), enabling direct comparison and quantification of instrument-specific drift. Over such short timescales, the drift was well-approximated by a linear trend

$$\Delta_{\text{sg}}(t_0 + \Delta t) = k_{\text{sg}} \Delta t. \quad (2)$$

Both the drift rate and the offset of each spring gravimeter were determined by fitting the calibration data to simultaneous atomic measurements. This nightly calibration effectively removed short-term drift and stabilized the instruments' local reference points, as illustrated in Fig. (2a,b). After tidal correction, the atomic gravimeter measurements, Fig. (2c), exhibit a gradual increase of approximately 50  $\mu\text{Gal}$  over the survey period. This slow trend likely reflects environmental and regional gravity variations beyond solid Earth tides, predominantly due to ocean loading given the survey's coastal island location [2]. Because the nightly calibration is tied directly to the atomic reference, these long-term varia-

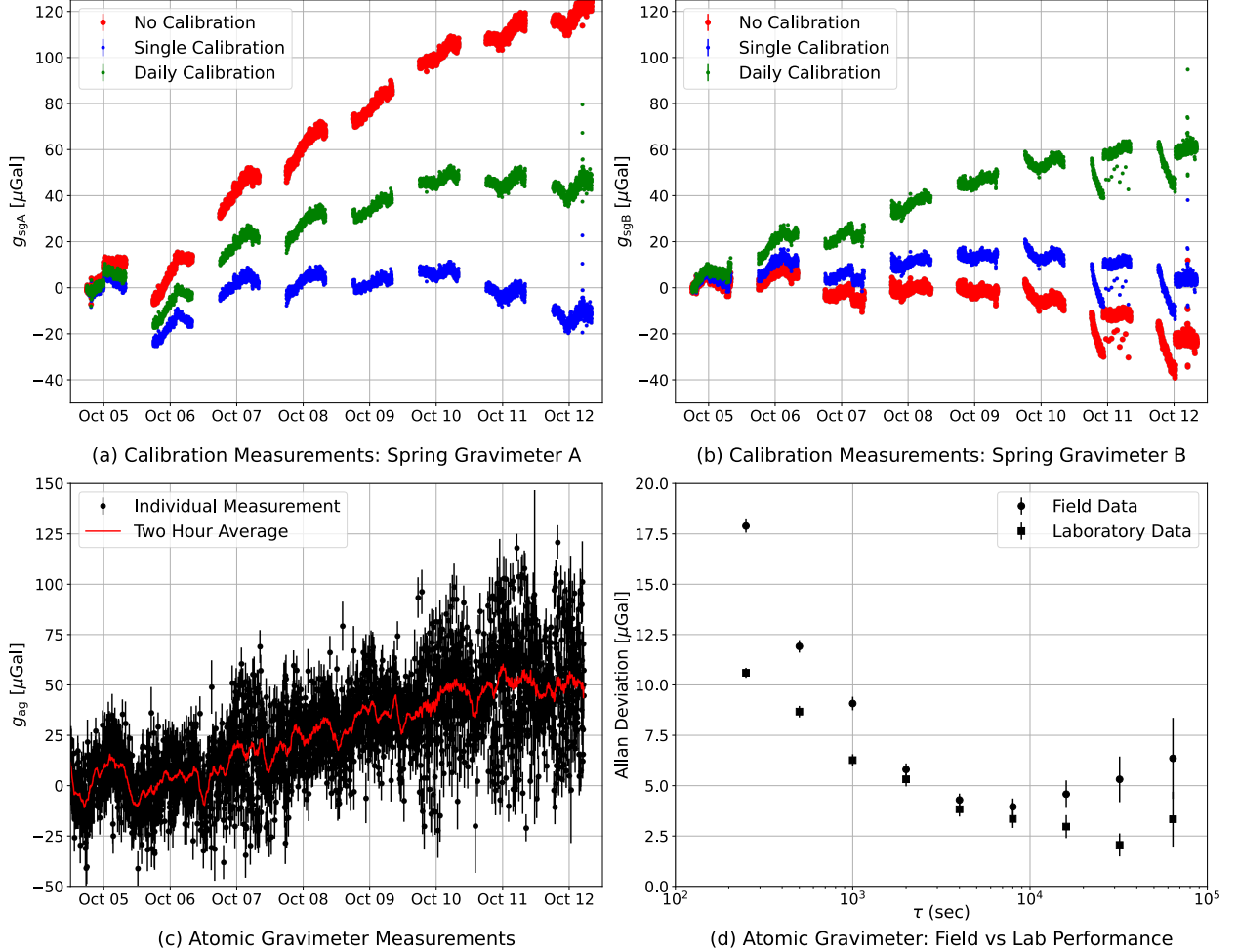


FIG. 2. Overnight calibration data for the two spring gravimeters,  $g_{sgA}$  (a) and  $g_{sgB}$  (b), compared against continuous absolute gravity measurements from the atomic gravimeter  $g_{ag}$  (c), collected over eight days. Each spring gravimeter panel shows uncorrected data (red), a single global drift correction from the start of the survey (blue), and daily drift corrections derived from the atomic reference (green). All data are tide-corrected and plotted as relative gravity to emphasize temporal variations. The daily calibration accurately tracks the gradual 50  $\mu\text{Gal}$  increase observed by the atomic gravimeter, while the single global correction does not. A brief discontinuity in  $g_{sgB}$  near the end of the survey resulted from a power interruption and was corrected during processing. Panel (d) shows the Allan deviation of the atomic gravimeter measurements in the field (circles) compared with laboratory data over a similar timescale (squares), demonstrating comparable long-term stability with slightly elevated white-noise levels in the field due to environmental vibrations and tilt.

tions are naturally incorporated into the spring gravimeter's temporal corrections. By contrast, a single global calibration based solely on the initial reference period fails to capture this evolving baseline, producing a systematic bias that grows over the course of the survey.

Although the atomic gravimeter exhibited high overall stability, a distinct offset was observed between 3 and 4 October 2023, likely due to mechanical settling of the container floor, consistent with previous field observations [20]. This shift was excluded from the calibration



FIG. 3. Field gravity measurements colored by PPK solution quality. Green points correspond to fully converged solutions with  $<10$  cm vertical uncertainty. Blue points indicate partially converged solutions that provided usable elevation estimates despite larger or less well-defined uncertainties. Orange points mark locations where the PPK algorithm did not produce a usable solution; these stations were excluded from elevation-dependent analyses.

of the spring gravimeters. Following this initial adjustment, the instrument remained stable for the remainder of the survey. To quantify performance, the Allan deviation of the atomic gravimeter was evaluated under both field and laboratory conditions over similar time spans, Fig. (2d). Laboratory data, collected under rigid mounting and tightly controlled environmental conditions, achieved a noise floor of approximately  $2\text{ }\mu\text{Gal}$ . During the survey, the minimum Allan deviation was  $4\text{ }\mu\text{Gal}$ , increasing beyond integration times of 4 hours (15000 s) as flicker noise began to dominate. These results confirm that the atomic gravimeter maintained sufficient long-term stability to support daily in situ calibration, even under variable environmental conditions.

### Elevation Correction

The effect of elevation  $h$  at position  $\vec{x}$ , on the measured gravity signal can be separated into three components [1, 34]:

- Free-air correction,  $g_f(\vec{x}) = 0.3086 \text{ mGal/m} \times h$ ,

which compensates for the decrease in gravitational acceleration with increasing elevation above the reference level.

- Bouguer correction,  $g_b(\vec{x}) = 0.04193 \text{ mGal}/(\text{m} \cdot \text{g/cm}^3) \times \rho h$ , which restores the gravitational effect of the rock mass between the measurement point and the reference elevation, assuming a uniform subsurface density  $\rho$ .
- Terrain correction,  $g_t(\vec{x})$ , which accounts for local topographic deviations from the idealized infinite slab assumed in the Bouguer approximation.

The net elevation correction is therefore given by

$$\delta_z g(\vec{x}) = g_f(\vec{x}) - g_b(\vec{x}) + g_t(\vec{x}). \quad (3)$$

In this study  $g_t(\vec{x})$  is neglected due to the limited availability of high-resolution topographic data. This omission is not expected to obscure broader gravity trends because the survey area exhibits low relief, and the resulting uncertainty is well below the measurement precision

Accurate elevation correction depends on reliable vertical positioning. The distribution of field gravity stations by PPK solution quality is shown in Fig. (3). Of the 262 field measurements, 59 yielded fully converged PPK solutions with vertical uncertainties below 10 cm, corresponding to a gravity uncertainty of  $\sim 10\mu\text{Gal}$ . These high-precision points provide the elevation control necessary to validate the drift corrections described in the previous subsection. An additional 127 stations produced partially converged PPK solutions with larger and less well-defined vertical uncertainties; while these carry more uncertainty, they still capture the spatial gravity variations across the survey area and are retained for analysis. Stations for which the PPK solution failed to converge were excluded from the elevation-dependent analysis.

## RESULTS

The final gravity map, corrected for tidal, instrumental, and elevation effects, is shown in Fig. (4). Gravity values are referenced to the mean value recorded at the atomic gravimeter site, with the resulting field

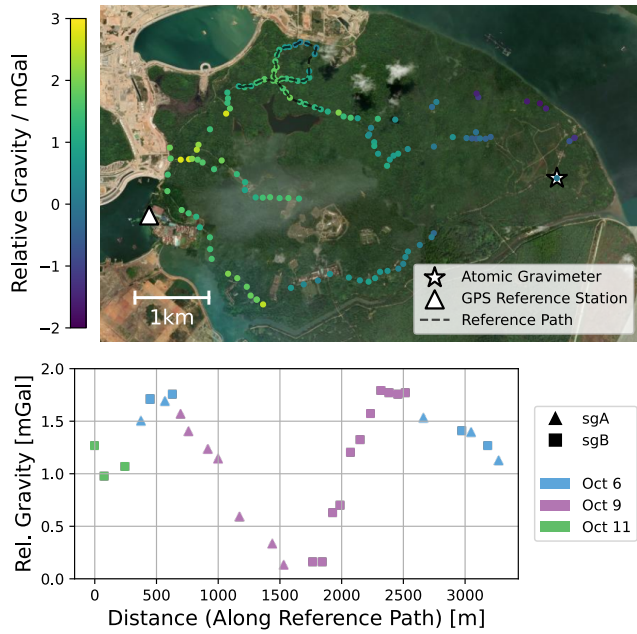


FIG. 4. *Top*: Gravity distribution across the survey after applying temporal and elevation corrections to all stations with a usable PPK solution. *Bottom*: Gravity measurements along the reference path with corresponding high-precision elevation data. Distance 0 corresponds to the westernmost point of the path; upon reaching the junction, the path follows a counterclockwise loop before continuing east. Markers indicate the specific instrument (triangle: spring gravimeter A; square: spring gravimeter B), and colors correspond to the survey day. The profile demonstrates temporal consistency across repeated measurements and reveals a gradual gradient along the path.

spanning approximately -2 mGal to +3 mGal across the survey area. A coherent northeast–southwest gradient is observable across the dataset, which may reflect underlying geological variations. This large-scale pattern demonstrates that the hybrid survey captured spatially meaningful variations in the gravitational field, even when including stations with reduced vertical precision, and highlights the capability of field-deployed quantum sensors to provide a stable reference for high-precision measurements.

Along a well-sampled reference path within the survey area, many stations yielded fully converged PPK solu-

tions, providing high-precision gravity measurements after drift and elevation correction. These measurements were collected over several days and using both spring gravimeters, enabling robust cross-comparison and validation of the atomic-gravimeter-based drift correction. The resulting gravity profile along this path exhibits a gradual change consistent with the overall trend observed across the survey area. Notably, the looped segment of the path, completed entirely on October 9 with measurements shared between the two spring gravimeters, aligns closely with observations from October 6 at the junction of the reference path, providing additional confirmation of temporal stability. Small residual deviations remain, likely arising from unmodeled instrumental or environmental effects, but the overall pattern demonstrates that the methodology can reliably capture multi-day spatial variations using field-deployed quantum-enabled gravimeters.

Residual deviations between neighboring stations, typically on the order of 100–500  $\mu$ Gal, are primarily associated with partially converged PPK solutions, which provide less certain elevation data and therefore introduce uncertainty into the gravity corrections. Additional site-dependent effects—including minor soil compaction during measurement, local variations in near-surface density not captured by the uniform Bouguer correction, and environmental influences during deployment—also contribute to the observed scatter. A small fraction of these secondary effects impacted some of the high-precision GPS-supported measurements, introducing additional deviations not explicitly accounted for in the correction model. Importantly, these residuals remain small relative to the regional gravity gradient and do not compromise the interpretation of broader spatial patterns.

## DISCUSSION

This survey represents a significant milestone in field-deployable quantum gravimetry. By combining a containerized atomic gravimeter with mobile spring instruments, we demonstrated that absolute, quantum-grade accuracy can be extended across a large-area field survey. Instrument drift was mitigated through on-site daily calibration, enabling asynchronous cross-

comparisons between independent gravimeters and allowing high-precision measurements over multiple days. The atomic gravimeter maintained high stability throughout the campaign, including after minor initial mechanical settling of the container floor, confirming its suitability as a reliable field reference. All quantum hardware was housed in a single air-conditioned shipping container, which preserved laboratory-class sensitivity for over two weeks, see Fig. (2d), despite tropical climate conditions and environmental noise, demonstrating the system's operational robustness.

By leveraging this quantum-referenced hybrid approach, mobile spring gravimeters were able to capture robust gravity variations across a large spatial area and extended timescale. Fully converged PPK stations provided high-precision control, while partially converged stations still contributed to mapping broader trends, despite limitations in GPS-based elevation accuracy due to dense canopy and intermittent satellite coverage. The containerized atomic gravimeter serves as an on-site absolute reference, enabling conventional relative instruments to achieve traceable, quantum-grade precision in challenging field conditions. This methodology illustrates how field-deployed atomic sensors can extend quantum-level stability to large-area surveys, providing a scalable model for high-resolution gravity mapping. Next-generation platforms under development aim to reduce mobilisation time, integrate autonomous tilt control, and enable cloud-based data processing, further broadening access to precision, quantum-enabled gravimetry for applications in hydrology, natural hazard monitoring, resource prospecting, and environmental change detection.

---

<sup>†</sup> These authors contributed equally to this work.

- [1] W. J. Hinze, R. Von Frese, and A. H. Saad, *Gravity and magnetic exploration: Principles, practices, and applications* (Cambridge University Press, 2013).
- [2] M. Van Camp, O. de Viron, A. Watlet, B. Meurers, O. Francis, and C. Caudron, Geophysics from terrestrial time-variable gravity measurements, *Reviews of Geophysics* **55**, 938 (2017).
- [3] F. Flechtner, C. Reigber, R. Rummel, and G. Balmino, Satellite gravimetry: a review of its realization, *Surveys in Geophysics* **42**, 1029 (2021).
- [4] T. R. LaFehr and M. N. Nabighian, *Fundamentals of gravity exploration* (Society of Exploration Geophysicists, 2012).
- [5] T. Niebauer, Gravimetric methods – absolute and relative gravity meter: Instruments concepts and implementation (Elsevier, 2015) pp. 37–57.
- [6] K. Davis, Y. Li, and M. Batzle, Time-lapse gravity monitoring: A systematic 4d approach with application to aquifer storage and recovery, *Geophysics* **73**, WA61 (2008).
- [7] E. Groten and M. Becker, Methods and experiences of high precision gravimetry as a tool for crustal movement detection, *Journal of geodynamics* **19**, 141 (1995).
- [8] L. Timmen, O. Gitlein, V. Kleemann, and D. Wolf, Observing gravity change in the fennoscandian uplift area with the hanover absolute gravimeter, *Pure and applied geophysics* **169**, 1331 (2012).
- [9] L. LaCoste, The zero-length spring gravity meter, *The Leading Edge* **7**, 20 (1988).
- [10] A. Okiwelu, E. Okwueze, and I. Osazuwa, Strategies for accurate determination of drift characteristics of unstable gravimeter in tropical, coastal environment, *Applied Physics Research* **3**, 190 (2011).
- [11] M. Schilling and O. Gitlein, Accuracy estimation of the ife gravimeters micro-g lacoste gphone-98 and zls burris gravity meter b-64, in *IAG 150 Years: Proceedings of the IAG Scientific Assembly in Postdam, Germany, 2013* (Springer, 2015) pp. 249–256.
- [12] P. Gillot, O. Francis, A. Landragin, F. P. Dos Santos, and S. Merlet, Stability comparison of two absolute gravimeters: optical versus atomic interferometers, *Metrologia* **51**, L15 (2014).
- [13] M. Kasevich and S. Chu, Atomic interferometry using stimulated raman transitions, *Physical review letters* **67**, 181 (1991).
- [14] A. Peters, K. Y. Chung, and S. Chu, Measurement of gravitational acceleration by dropping atoms, *Nature* **400**, 849 (1999).
- [15] V. Ménoret, P. Vermeulen, N. Le Moigne, S. Bonvalot, P. Bouyer, A. Landragin, and B. Desruelle, Gravity measurements below 10–9 g with a transportable absolute quantum gravimeter, *Scientific reports* **8**, 12300 (2018).
- [16] C. Ruan, W. Zhuang, J. Yao, Y. Zhao, Z. Ma, C. Yi, Q. Tian, S. Wu, F. Fang, and Y. Wen, A transportable atomic gravimeter with constraint-structured active vibration isolation, *Sensors* **24**, 2395 (2024).
- [17] B. Wu, Z. Wang, B. Cheng, Q. Wang, A. Xu, and Q. Lin, The investigation of a  $\mu$ gal-level cold atom gravimeter for field applications, *Metrologia* **51**, 452 (2014).
- [18] Y. Bidel, O. Carraz, R. Charrière, M. Cadoret, N. Zazham, and A. Bresson, Compact cold atom gravimeter for field applications, *Applied Physics Letters* **102**

(2013).

[19] F. A. Narducci, A. T. Black, and J. H. Burke, Advances toward fieldable atom interferometers, *Advances in Physics: X* **7**, 1946426 (2022).

[20] N. Shettell, K. S. Lee, F. E. Oon, E. Maksimova, C. Hufnagel, S. Wei, and R. Dumke, Geophysical survey based on hybrid gravimetry using relative measurements and an atomic gravimeter as an absolute reference, *Scientific Reports* **14** (2024).

[21] L. Chen-yang, X. Ru-gang, C. Xi, S. Hong-bo, L. Su-peng, L. Yu, H. Ming-qi, D. Xue-feng, L. Zhao-long, X. Wei-peng, *et al.*, Joint gravity survey using an absolute atom gravimeter and relative gravimeters, arXiv preprint arXiv:2504.00588 (2025).

[22] M. Sugihara and T. Ishido, Geothermal reservoir monitoring with a combination of absolute and relative gravimetry, *Geophysics* **73**, WA37 (2008).

[23] J. Nishijima, C. Umeda, Y. Fujimitsu, J. Takayama, N. Hiraga, and S. Higuchi, Repeat absolute and relative gravity measurements for geothermal reservoir monitoring in the ogiri geothermal field, southern kyushu, japan, in *IOP Conference Series: Earth and Environmental Science*, Vol. 42 (IOP Publishing, 2016) p. 012004.

[24] F. Greco, G. Currenti, G. D'Agostino, A. Germak, R. Napoli, A. Pistorio, and C. Del Negro, Combining relative and absolute gravity measurements to enhance volcano monitoring, *Bulletin of volcanology* **74**, 1745 (2012).

[25] S. Zerbini, M. Negusini, C. Romagnoli, F. Domenichini, B. Richter, and D. Simon, Multi-parameter continuous observations to detect ground deformation and to study environmental variability impacts, *Global and Planetary Change* **34**, 37 (2002).

[26] O. Francis, T. Niebauer, G. Sasagawa, F. Klopping, and J. Gschwind, Calibration of a superconducting gravimeter by comparison with an absolute gravimeter fg5 in boulder, *Geophysical Research Letters* **25**, 1075 (1998).

[27] Y. Imanishi, T. Higashi, and Y. Fukuda, Calibration of the superconducting gravimeter t011 by parallel observation with the absolute gravimeter fg5# 210—a bayesian approach, *Geophysical Journal International* **151**, 867 (2002).

[28] T. Niebauer, R. Billson, B. Ellis, B. Mason, D. van Westrum, and F. Klopping, Simultaneous gravity and gradient measurements from a recoil-compensated absolute gravimeter, *Metrologia* **48**, 154 (2011).

[29] S. Merlet, P. Gillot, B. Cheng, R. Karcher, A. Imanaliev, L. Timmen, and F. Pereira dos Santos, Calibration of a superconducting gravimeter with an absolute atom gravimeter, *Journal of Geodesy* **95**, 62 (2021).

[30] A. Hugill, Scintrex cg-3 automated gravity meter: description and field results, in *SEG Technical Program Expanded Abstracts 1990* (Society of Exploration Geophysicists, 1990) pp. 601–604.

[31] D. A. Chapin, The theory of the bouguer gravity anomaly: A tutorial, *The Leading Edge* **15**, 361 (1996).

[32] M. Mikolaj and B. H  bel, The first tidal analysis based on the cg-5 autograv gravity measurements at modra station, *Contributions to Geophysics and Geodesy* **43**, 59 (2013).

[33] G. Jentzsch, Earth tides and ocean tidal loading, *Tidal phenomena* , 145 (2005).

[34] W. M. Telford, L. P. Geldart, and R. E. Sheriff, *Applied geophysics* (Cambridge university press, 1990).

*Acknowledgements* - This research is supported by the NRF through NRF2021-QEP2-03-P06. The authors would like to thank Johnathan Kim, for organizing the logistics of the geophysical survey, Aveek Chandra, Gan Koon Siang, Christoph Hufnagel and Paul Tan for assisting with the gravity measurements as well as, Maung Maung Phy, Yukuan Chen, Yu Jiang, Nurdin Elon Dahlan, and Shengji Wei for assisting with preparations of the geophysical survey, and Jan Mrlina for the insightful discussions on geology.

*Author Contributions* - N.S. and K.S.L. conducted the data analysis. K.S.L., F.E.O., E.M., H.H.C. and R.D. conducted the data collection during the survey. F.E.O. operated the atomic gravimeter. R.D. conceived the project. N.S., K.S.L., and R.D. contributed to the writing of the manuscript.

*Data Availability* - Raw data captured from the relative gravimeter, absolute gravimeter, and gps during the survey, can be provided upon reasonable request.

*Competing Interests* - The authors have no conflicts to disclose.